HHS Public Access

Author manuscript

Circ Arrhythm Electrophysiol. Author manuscript; available in PMC 2016 October 01.

Published in final edited form as:

Circ Arrhythm Electrophysiol. 2015 October ; 8(5): 1219–1227. doi:10.1161/CIRCEP.115.003070.

Molecular Mapping of Sinoatrial Node HCN Channel Expression in the Human Heart

Ning Li, MD, PhD[1], **Thomas A. Csepe, BSc**[1], **Brian J. Hansen, BSc**[1], **Halina Dobrzynski, PhD**[2], **Robert S.D. Higgins, MD**[3], **Ahmet Kilic, MD**[3], **Peter J. Mohler, PhD**[1], **Paul M.L. Janssen, PhD**[1], **Michael R. Rosen, MD**[4], **Brandon J. Biesiadecki, PhD**[1], and **Vadim V. Fedorov, PhD**[1]

[1]Department of Physiology & Cell Biology and Dorothy M. Davis Heart & Lung Research Institute, The Ohio State University Wexner Medical Center, Columbus, OH

[2]Institute of Cardiovascular Sciences, University of Manchester, Manchester, United Kingdom

[3]Department of Surgery and Dorothy M. Davis Heart & Lung Research Institute, The Ohio State University Wexner Medical Center, Columbus, OH

[4]Departments of Pharmacology and Pediatrics, Columbia University, New York, NY

Abstract

Background—The hyperpolarization-activated current, I_f, plays an important role in sinoatrial node (SAN) pacemaking. Surprisingly, the distribution of Hyperpolarization-activated Cyclic Nucleotide-gated (HCN) channels in human SAN has only been investigated at the mRNA level. Our aim was to define the expression pattern of HCN proteins in human SAN and different atrial regions.

Methods and Results—Entire SAN complexes were isolated from failing (n=5) and non-failing (n=9) human hearts cardioplegically-arrested in the operating room. Three dimensional intramural SAN structure was identified as the fibrotic compact region around the SAN artery with Connexin43-negative pacemaker cardiomyocytes visualized in Masson's trichrome and immunostained cryosections. SAN protein was precisely isolated from the adjacent frozen SAN tissue blocks using a 16G biopsy needle. The purity of the SAN protein was confirmed by Connexin43 immunoblot. All three HCN isoform proteins were detected in SAN. HCN1 was predominantly distributed in the human SAN with a 125.1±40.2 (n=12) expression ratio of SAN to right atrium (RA). HCN2 and HCN4 expression levels were higher in SAN than atria with SAN to RA ratios of 6.1±0.9 and 4.6±0.6 (n=12), respectively.

Conclusions—This is the first study to conduct precise 3D molecular mapping of the human SAN by isolating pure pacemaker SAN tissue. All three cardiac HCN isoforms had higher expression in the SAN than the atria. HCN1 was almost exclusively expressed in SAN,

Correspondence: Vadim V. Fedorov, PhD, Department of Physiology and Cell Biology, The Ohio State University Wexner Medical Center, 300 Hamilton Hall, 1645 Neil Avenue, Columbus OH 43210, Tel: 1-614-292-5154, Fax: 1-614-252-4888, vadim.fedorov@osumc.edu / fedorov.2@osu.edu.

Conflict of Interest Disclosures: None

emphasizing its utility as a new specific molecular marker of the human SAN and as a potential target of specific treatments intended to modify sinus rhythm.

Keywords

Sinoatrial node; HCN channel; Sinus node dysfunction; Heart failure; Human heart

Introduction

The spontaneous electrical activity of mammalian hearts arises from specialized cardiomyocytes of the sinoatrial node (SAN)[1]. Multiple ion channels and Ca^{2+}-handling proteins are essential for generation of the SAN action potential[2]. Among these, the hyperpolarization-activated "funny" current (I_f) is a major determinant of cardiac diastolic depolarization and plays a key role in controlling heart rate[3]. Hyperpolarization-activated Cyclic Nucleotide-gated (HCN) channels are coded by four genes (*HCN1-4*), representing the molecular α-subunits of native I_f channels.

The rarity of human SAN specimens available for research and the complex intramural structure of the human SAN[4, 5] have resulted respectively in the lack of reliable means to acquire and accurately localize SAN samples. Thus, there remain critical barriers to study the molecular profile of the SAN in normal and diseased human hearts. Studies at the mRNA level indicate that the most highly-expressed HCN subtype in the mammalian SAN is HCN4[6-8], which has been considered to be crucial for the generation of the heart beat and maturation of pacemaker type cells during embryogenesis[9]. Species-dependent expression of HCN1 and HCN2 has also been reported in the SAN[6-8], and a recent study reports HCN1 also contributes to stable heart rate in mouse SAN[10]. Heart failure (HF) results in significant SAN remodeling and dysfunction[11]. Studies on rabbit[12] and dog[7] SAN suggest that HF-induced SAN dysfunction is at least in part attributable to remodeling of I_f and down-regulation of both HCN4 and HCN2. However, experimental data on the molecular characteristics of human SAN is minimal. Verkerk et al[13] showed the presence of I_f in human SAN myocytes isolated from a single human heart with history of inappropriate SAN tachycardia, and in other studies *HCN4* loss-of-function mutations have been associated with SAN dysfunction[14] and cardiomyopathy[15]. Although HCN1, HCN2 and HCN4 mRNAs have been detected in non-failing human SAN[8], no data about protein distribution of all 3 HCN isoforms in human SAN is available. In the present study, we precisely isolated protein from SAN pacemaker clusters and adjacent atrial tissues of cardioplegically-arrested human hearts to investigate the expression patterns of HCN1, HCN2, and HCN4. For the first time, we identified the distinct and specific expression of HCN1 protein in human SAN. Our findings suggest a potentially important contribution of HCN1 to human SAN pacemaking.

Methods

SAN and atrial tissue collection

De-identified, coded human hearts were obtained from Lifeline of Ohio Organ Procurement Organization and the Division of Cardiac Surgery at The OSU Wexner Medical Center

(Table 1). This study was approved by The Ohio State University Institutional Review Board (IRB).

Explanted human hearts (n=14) were obtained in the operating room at the time of cross-clamp and immediately preserved with ice cold cardioplegic solution and stored at 4°C during transport and dissection as previously described[16]. Hearts were transported to the experimental lab within 15 minutes; whole intact atria were dissected from ventricles and coronary-perfused with oxygenated cardioplegic solutions at 4°C to prevent any potential tissue degradations due to ischemia.

Twelve fresh human SAN with adjacent atrial tissues (Hearts #1-12) were pinned to silicone pads (Figure 1), embedded in O.C.T. (Fisher Scientific), frozen in cold isopentane and stored at −80°C until use. The pins were visible markers used to indicate the orientation of the embedded SAN during subsequent dissection. Based on anatomic and functional data[4,5], frozen SAN tissues (cryo blocks) were cut into head, center and tail blocks (~4-6 mm long), respectively perpendicular to epicardium (Figure 1). In keeping with previous studies[4, 17-19], we describe the most superior third of the SAN as the ‘‘head’’, the middle third as the ‘‘center’’, and the inferior third as the ‘‘tail’’ (Figure 1A). Cryosections were collected from both ends of the cryo blocks at 20μm thickness. Masson’s trichrome staining and Connexin43 (Cx43)/α-actinin double immunolabeling were performed on cryosections. Histology and immunostaining images were used to guide the SAN tissue collection from cryo block. 16G (1.3mm I.D.) biopsy needles were used to accurately collect SAN tissue along, but not including, the main artery within the Cx43-negative area from the SAN head, center and tail separately. According to the size of the Cx43 negative tissue, 2-3 punches (10~15mg in total) of pure SAN tissue could be collected from each cryo block. Tissue from the crista terminalis (CT), interatrial septum (IAS) and right atrial free wall (RAFW) were also collected from the same cryo block from which the SAN center was collected using the same method. Separate samples of the atrial tissue, such as left atrial free wall, left atrial appendage, right atrial appendage (RAA), right atrioventricular ring (RR)[2], and different locations of the RAFW (superior, middle and inferior) were collected fresh and flash-frozen in liquid nitrogen during heart dissection. Additionally, two SAN preparations (Hearts #13 and #14) immediately after cardioplegic arrest were fixed in 4% paraformaldehyde, paraffin-embedded and sectioned at 5 μm thickness parallel to the epicardium for histology and immunostaining.

Histology

Cryosections were fixed in 4% paraformaldehyde for 1 hour and stained with Masson’s trichrome (Sigma Aldrich), as described previously[4]. Images were taken with a 20x digital slide scanner (0.5×0.5μm^2 resolution, Aperio ScanScope XT, Leica).

Immunohistochemistry

Cryosections were fixed with −20°C methanol for 5min before immunostaining. Sections were permeabilized with 0.1% Triton X-100 (Sigma Aldrich), blocked with 1% bovine serum albumin, and incubated with primary antibodies overnight at 4°C. The following day, sections were incubated in secondary antibodies for 2 hours at room temperature and

mounted in ProLong® Gold Antifade Mountant with DAPI (Life Technologies). The primary and secondary antibodies include: mouse anti-HCN1 (1:100, Abcam), rat anti-HCN4 (1:100, Abcam), rabbit anti-HCN2 (1:100, Alamone), rabbit anti-Cx43 (1:400, Sigma-Aldrich), mouse anti-α-actinin (1:200, Abcam), goat anti-rabbit Alexa Fluor 488 (1:200, Life Technologies), and goat anti-mouse Alexa Fluor 568 (1:200, Life Technologies). Paraffin sections were dewaxed and heated in citrate-based buffer for antigen retrieval before the immunostaining protocol. Sections were imaged using an Olympus FV1000 Filter confocal microscope and florescence density was measured by ImageJ software. A summary of antibodies used in immunohistochemistry protocols is provided in Supplemental Table I, and the specificity of antibody is discussed in Supplemental Material (Supplemental Figure I).

Immunoblot analysis

For protein isolation, human SAN and atrial tissue were homogenized in 2x urea buffer[20] (10μl buffer per 1mg tissue) followed by centrifugation at 14,000 rpm for 10 min at 10°C, and the supernatant was collected. Protein yield was quantified using RCDC protein assay (Bio-rad). Equal amounts (20μg/sample) of proteins were separated by SDS-PAGE 12% (200:1) polyacrylamide gels and transferred to 0.45μM low fluorescence PVDF membrane by methods previously described[20]. After blocking, membranes were incubated with various primary antibodies overnight at 4°C: mouse anti-HCN1 (1:500, Abcam), rat anti-HCN4 (1:100, Abcam), rabbit anti-HCN2 (1:500, Alamone), and rabbit anti-Cx43 (1:8,000, Sigma-Aldrich). Mouse anti-GAPDH (1:20,000, Sigma-Aldrich) was used as reference for equal protein loading and to normalize HCN channel protein band intensity. Subsequently, 1:2,000 diluted fluorescent DyLight conjugated secondary antibodies (Jackson ImmunoResearch Laboratories) were applied to membranes for 1 hour at room temperature. The specific bands were detected on a Typhoon 9410 imager (GE Healthcare) and quantified by densitometry analysis (ImageQuant, GE Healthcare).

Statistical analysis

Data are presented as Mean±SEM. To test if protein expression ratios of SAN to RAFW and RR to RAFW were different from 1, ratios for each heart were log10 transformed for each protein to stabilize variance and the two-tailed one-sample t-test was applied (Supplemental Table II). The two-tailed Satterthwaite t-test was used to evaluate the difference between failing and non-failing groups (Supplemental Table III). All tests were done using R 3.1.0 for Windows. A p-value of 0.05 or below was considered significant.

Results

Localization and extraction of human SAN tissue

The SAN is located at the junction of the superior vena cava (SVC) and right atrium (RA) in the human heart. Figure 1A illustrates the anatomical and functional boundaries of the human SAN. The intramural SAN structure was identified in the histology images as the region of dense fibrotic matrix surrounding and isolating clusters of specialized cardiomyocytes around the SAN artery (Figure 1B, middle). Gap junction protein Cx43 is known to be absent from the SAN but abundantly expressed in the RA of humans and small

mammals[8, 21]. Figure 1B shows a positive correlation between the histologically-identified SAN and the SAN identified by negative Cx43 expression in the present study. SAN, CT and RAFW tissue were collected from the locations indicated by the pink dots in Figure 1B. The average yield of total SAN protein was roughly 200-300μg from each SAN cryo block. Immunoblots, performed with HCN4, α-actinin and Cx43 antibodies, detected specific bands at the expected molecular weights (~150, 100 and 43kDa, respectively). Alpha-actinin and GAPDH expression were comparable in all tested samples. Cx43 expression was markedly lower in the SAN center than in CT and RAFW tissue, while HCN4 expression was higher in the SAN center than in the adjacent tissues (Figure 1C). In all 12 hearts, total Cx43 expression was significantly lower in SAN tissue than in the RAFW, with GAPDH normalized band density ratio of SAN/RAFW=0.18±0.05 ($p<0.01$), which attests to the purity of the SAN sample[8, 11].

Expression pattern of HCN channels in human SAN and atria

Expression levels of the three HCN isoforms in human atria were determined by immunoblot and immunohistochemistry. First, the distribution of HCN isoforms within different areas of the human SAN was investigated. Figure 2 shows representative immunoblot results from Heart #2. The expression level of each HCN isoform was similar among the three SAN locations (head, center and tail) within this heart. As such, consecutive analysis used the SAN center to represent SAN expression. We further investigated the expression pattern of HCN channels in the human SAN center and the different atrial tissue. In all studied hearts, expressions of all three HCN isoforms in SAN center were always higher than in the RAFW. Figure 3 shows representative immunoblot results from Heart #6 and Figure 4 summarizes data from 12 individual SAN-atrial tissue preparations. All immunoblotting experiments comparing the HCN isoform expression levels between SAN and RAFW were repeated at least twice. In Figure 3A, a 90kDa band corresponding to the mature glycosylated HCN1 protein[10] can be seen in the SAN tissue, but other atrial tissues displayed bands of lesser density. The specific band density of HCN1 (GAPDH normalized) was 5.6 to 446 times greater in the SAN region than in the RAFW with the average ratio of SAN/RAFW=125.1±40.2 ($n=12$, $P<0.05$). An 85kDa band detected in all regions may represent a non-specific band as has been similarly observed in mouse HCN1 immunoblots[10]. Both HCN2 and HCN4 proteins were detected and quantified in the SAN and all other atrial tissue. HCN2 protein expression was 6.1±0.9 fold (2.4-12.5 times) more abundant in the SAN than in RAFW ($n=12$, $P<0.05$), and HCN4 protein expression was 4.6±0.6 fold (2.2-8.3 times) higher in the SAN than in the RAFW ($n=12$, $P<0.05$). We also found HCN2 expression in the RR area was significantly higher than in the RAFW, with a band density ratio of RR/RAFW=2.4±0.4 ($n=12$, $p<0.05$). However, HCN1 and HCN4 protein expression showed no difference in the RR area compared to the RAFW (Supplemental Table II).

We also performed double-label immunostaining (HCN1/Cx43, HCN2/Vimentin, HCN4/Cx43) to demonstrate the cell-specific distribution of the three HCN channel proteins in a series of paraffin slides from Heart #13 and #14 (Figure 5). The SAN area was identified by the lack of expression of Cx43, as well as a dense matrix of fibroblasts labeled by

Vimentin[11]. For all HCN antibodies, we achieved specific staining of cardiomyocytes in the SAN and surrounding atrial regions.

HCN expression changes in heart failure

To assess whether the HCN isoform expressions were modified by HF, we compared the protein expression level in the SAN center and RAFW between non-failing (NF) and failing (HF) hearts (Figure 6). Exclusion criteria from the NF control group included pacemaker implantation and greater than 20 minutes of down time (temporal duration between cardiac arrest and CPR or advanced cardiac life support); thus, Hearts #7-9 were omitted from this group. The SAN center showed significantly more protein expression of all three HCN isoforms than RAFW in both NF and HF hearts. HCN1 expression in the SAN showed no significant difference between NF and HF groups, and each group had considerable variance (GAPDH-normalized band density: NF=153.7±59.6, n=4; HF=161.8±79.8, n=5, p=0.94). Figure 6 shows that HF Hearts #4 and #5 (ischemic HF) had significantly lower HCN1 expression than Heart #3 (non-ischemic HF) while HCN2 and HCN4 expression was still well-preserved in Heart #4 and #5. HCN1 expression (90kDa band) in the RAFW was at a very low level in all hearts. No significant changes in HCN2 and HCN4 expression were observed between NF (n=4) and HF (n=5) groups (Supplemental Table III).

Discussion

Methodological Innovations: molecular mapping of the human SAN pacemaker complex

The expression levels of HCN isoforms strongly depends on the cardiac region and varies among species[22]. As we described previously[4, 5], the human SAN has a complex transmural 3D structure and the leading pacemaker sites are located at the center and close to the junction of the center and tail thirds of the SAN. Considering the variation in size and intramural location of SAN in individual heart preparations when comparing expression levels of HCN protein in SAN to those in adjacent atrial tissue, we only used SAN protein isolated from the SAN center. In each heart preparation, specificity of SAN tissue extraction was confirmed by negative Cx43 expression before and after protein isolation using immunostaining and immunoblotting respectively. This study specifically determined HCN expression in “pure” SAN tissue that was not “contaminated” by surrounding atrial tissue; therefore, our results can be relied on to show the actual difference between SAN and the adjacent atrial tissue. We suggest that this novel approach provides a reproducible method for specific tissue isolation to study the molecular profiles of the human SAN and other specific cardiac tissues in normal and pathologic conditions.

The potential function of HCN in pacemaking

The functional relevance of I_f/HCN channels in the human cardiac pacemaker has been confirmed by the following: 1) specific blockade of I_f channels directly decreases heart rate with limited cardiovascular side effects[23, 24]; 2) *HCN4* gene mutations are associated with various inheritable forms of sinus arrhythmias[14]. This in no way diminishes the relevance of other mechanisms to SAN pacing[25]; however, our study focused on the HCN channel.

HCN4 is reported to be the most abundant HCN isoform in the mammalian SAN, suggesting that it plays a key role in the generation of primary pacemaker potentials. In mouse SAN, HCN4 mRNA represents nearly 60% of the HCN expression, followed by HCN1 (34%)[26]. The relative abundance of HCN mRNA measured in the human SAN (mRNAs HCN4/HCN1 ~6.3; HCN4/HCN2 ~33.8)[8] are similar to results in the rabbit SAN (mRNAs HCN4/HCN1=7.4 and HCN4/HCN2=46.4)[27]. Recent immunolabeling studies by Dobrzynski and colleagues[28] suggest that HCN4 cannot be an exclusive marker to map or identify the human SAN. These observations emphasize the differences in HCN isoform distribution between human and small mammals; in the latter, HCN4 is primarily expressed in the pacemaker conduction system[21, 27]. Multiple HCN isoforms may contribute to the assembly of heteromeric native cardiac I_f channels or to a mixed population of homomeric channels in the pacemaker cells[26]. In agreement with these studies, we found that expression of all HCN isoforms is higher in the SAN than in the surrounding atria, especially HCN1.

Compared to HCN4, the available literature on HCN1 is limited and inconsistent. Despite the detection of HCN1 mRNA in the adult heart, most studies report the absence of HCN1 protein in the SAN and whole heart[21, 27]. A few recent studies confirmed the high expression of HCN1 protein co-localized with HCN4 in the mouse SAN and indicated the significant contribution of HCN1 to native I_f [10, 26]. A mouse HCN1 knockout study[10] demonstrated that HCN1 could be important for stability of sinus rhythm. Our study demonstrates that HCN1 is primarily distributed in the SAN pacemaker and its expression in the surrounding right atrium is negligible, potentially reflecting a specific contribution of HCN1 to pacemaker current in the human SAN. This finding that HCN1 is high in SAN but minimal in atrial tissue may explain why previous reports investigating HCN1 in total atrial tissue underestimates the level of HCN1 specifically in the SAN. The expression pattern of HCN1 suggests that HCN1 could be an additional selective marker for normal SAN cells. Although we have suggested multiple anatomical landmarks demarcating the SAN in previous studies[4, 5], these landmarks (Cx43, fibrosis, fat) are only observed in histological or immunostaining analysis. While 2D immunostaining of Cx43 clearly shows a SAN boundary from the rest of the atrial myocardium (Figure 1), immunoblot data of HCN1 levels show more significant expression differences in SAN vs atria than Cx43 or HCN4 (Figure 2).

There is evidence that HCN2 contributes to mouse SAN I_f current[29], although most studies report that HCN2 is the main isoform expressed in atrial and ventricular working myocytes in small mammals (rabbit, rat and mouse)[6, 26]. Consistent with these observations, we observed heterogeneous HCN2 distribution in SAN and adjacent atrial tissue, with 6 times higher expression in SAN than RAFW, and expression 2 times higher in latent atrial pacemaker (RR)[30] than non-pacemaker regions (RAFW). Studies in animals[30] and our preliminary optical mapping experiments[31] revealed nodal-type action potentials and ectopic activity in the RR region that were depressed by I_f blockade[31]. We suggest that HCN2 may be important for both primary (SAN) and latent (RR) pacemaker automaticity in the human heart.

It is well known that different isoforms of the HCN channel exhibit distinct activation kinetics and varied sensitivity to cyclic adenosine monophosphate (cAMP)[32]. The varied

expression pattern of multiple isoforms of HCN in different pacemakers of the heart may explain their differences in intrinsic rhythm due to the wide range of I_f activation thresholds[6]. The different ratios of HCN isoforms in SAN and latent pacemakers may also affect the regional pacemaker sensitivity to neurotransmitters and HCN channel blockers[6, 33, 34]. HCN1 has faster kinetics and a more positive activation threshold than either HCN2 or HCN4; also, HCN1 is much less responsive to cAMP than either HCN2 or HCN4[32, 35]. For this reason, a greater proportion of HCN1 channels may be activated at higher membrane potentials than HCN4 channels, even though total protein expression of HCN1 is much less than HCN4. Our results demonstrated the expression of HCN1 exclusively in the SAN, which may help to protect the leading pacemaker from hyperpolarization and stabilize the leading pacemaker of the SAN during adrenergic receptor stimulation or phosphodiesterase inhibition. However, these suggestions require direct experimental confirmation.

HCN3 mRNA expression was negligible in human SAN and atrial tissues[8]. For this reason, we did not include HCN3 in our current SAN study. However, mouse studies indicate the presence of HCN3 channel subtypes in ventricular myocytes[36-38]. No expression of HCN3 was found in the murine cardiac conduction tissues[35]. HCN3-deficient mice display normal cardiac pacemaker activity[37], but these mice have a specific defect in the repolarization of the ventricular action potential.

The role of altered HCN function during cardiac diseases

Among HCN channels, *HCN4* mutations have been clearly associated with human SAN dysfunction, atrial fibrillation and atrioventricular block[14]. In human atria, although the mRNA level of HCN4 was significantly decreased in chronic atrial fibrillation, the protein level of HCN4 was preserved or slightly increased, causing an increase of I_f[39]. This result suggests that protein expression and function are not always correlated with mRNA because of complicated post-transcriptional modification mechanisms. Thus, it is particularly important to obtain direct evidence of HCN protein expression or function in human SAN/atria in normal and dysfunctional conditions, as was done in our study.

Previous studies reported that both mRNA and protein of HCN2/4 were detected in human atria and their expression levels were augmented in specimens from patients with HF[40]. Our study revealed that HCN1 was predominantly expressed in all investigated SAN, although expression levels of SAN HCN1 between hearts was variable. Moreover, statistical analysis did not reveal significant differences in HCN isoform expression between NF and HF groups. This may be due to the small number of hearts analyzed, as well as specific disease variation within each group.

Study Limitations

We studied a limited number of SAN samples. To ensure the quality of the SAN protein, we did not use optically mapped SAN preparations for protein isolation, so there was no direct correlation between functional data and the HCN expression pattern. We isolated protein from the SAN tissue section instead of single SAN myocytes. Even though we avoided the main arteries when collecting SAN tissue, we could not exclude the possibility that HCN

expression was contaminated by non-cardiomyocytes in the SAN region. To prevent proteolysis, all heart preparations were transferred and dissected at 4°C. Although we did not observe proteolysis for the other proteins (Cx43, α-actinin and GAPDH) detected by immunoblotting in our study, it may be possible that the HCN proteins could be degraded during the procedures. The individual role of the HCN isoforms in I_f generation should be evaluated with specific blockers of individual HCN1 or HCN4 I_f channel isoforms in both tissue and single cells, which will be the focus of our future studies.

Potential Implications and Future Directions

Our study presents the first quantitative analysis of HCN protein distribution and prevalence in human SAN and atrial tissues. We hypothesize that not only HCN4 but HCN1 may play an important role in human SAN pacing and potentially contribute to the native I_f in the SAN pacemaker cells. Although there is no HCN1 gene mutation related to arrhythmias found in humans so far, it may be considered as another candidate gene for human SAN dysfunction scans. Several studies demonstrated that overexpression of the HCN genes in myocytes via gene delivery or implantation of stem cells with overexpressed HCN2 successfully induced automaticity of a biological pacemaker in different animal models[41, 42]. Due to the specificity of HCN1 to the human SAN, the role of the HCN1 isoform should be taken into consideration for gene selection when developing a biological pacemaker[34, 43], and as a potential target of specific drug treatments aimed to affect sinus rhythm.

Conclusions

Our molecular study of human SAN tissue demonstrates a distinct cardiac expression profile of individual HCN isoforms in the SAN center vs. atria. We found that HCN1 is primarily expressed in the human SAN rather than the atria. We also observed that HCN2 and HCN4 expression is about 4-6 times higher in the SAN than RAFW, but these isoforms are less SAN-specific than that of HCN1. Furthermore, the novel technique used to isolate SAN tissue in this study may pave the way for more comprehensive molecular and functional integrated studies of the human SAN.

Supplementary Material

Refer to Web version on PubMed Central for supplementary material.

Acknowledgments

We thank the Lifeline of Ohio Organ Procurement Organization and the Division of Cardiac Surgery at The OSU Wexner Medical Center for providing the explanted hearts. We thank Mr. Benjamin Canan and Mr. Eric Schultz (PMLJ lab) as well as Mr. Brandon Moore (VVF lab) for their help with tissue processing. We also thank Dr. Stanislav Zakharkin for his help in statistical data analysis and for critical review of the manuscript.

Funding Sources: This work was supported by NIH HL115580 (VVF), HL113084 (PMLJ), HL084583, HL083422, HL114383 (PJM) and by funding from the Dorothy M. Davis Heart and Lung Research Institute.

References

1. Boyett MR, Honjo H, Kodama I. The sinoatrial node, a heterogeneous pacemaker structure. Cardiovasc Res. 2000; 47:658–687. [PubMed: 10974216]
2. Dobrzynski H, Anderson RH, Atkinson A, Borbas Z, D'Souza A, Fraser JF, Inada S, Logantha SJ, Monfredi O, Morris GM, Moorman AF, Nikolaidou T, Schneider H, Szuts V, Temple IP, Yanni J, Boyett MR. Structure, function and clinical relevance of the cardiac conduction system, including the atrioventricular ring and outflow tract tissues. Pharmacol Ther. 2013; 139:260–288. [PubMed: 23612425]
3. DiFrancesco D. Funny channels in the control of cardiac rhythm and mode of action of selective blockers. Pharmacol Res. 2006; 53:399–406. [PubMed: 16638640]
4. Fedorov VV, Glukhov AV, Chang R, Kostecki G, Aferol H, Hucker WJ, Wuskell JP, Loew LM, Schuessler RB, Moazami N, Efimov IR. Optical mapping of the isolated coronary-perfused human sinus node. J Am Coll Cardiol. 2010; 56:1386–1394. [PubMed: 20946995]
5. Zhao J, Csepe TA, Lim P, Hansen BJ, Li N, Kalyanasundaram A, Mohler PJ, Janssen PML, Davies EA, Weiss R, Fedorov VV. Detailed 3D reconstruction of the optically mapped sino-atrial node unravels direct evidence of specialized conduction pathways in the human heart. Heart Rhythm. 2014; 11:s102.
6. Shi W, Wymore R, Yu H, Wu J, Wymore RT, Pan Z, Robinson RB, Dixon JE, McKinnon D, Cohen IS. Distribution and prevalence of hyperpolarization-activated cation channel (HCN) mRNA expression in cardiac tissues. Circ Res. 1999; 85:e1–e6. [PubMed: 10400919]
7. Zicha S, Fernandez-Velasco M, Lonardo G, L'Heureux N, Nattel S. Sinus node dysfunction and hyperpolarization-activated (HCN) channel subunit remodeling in a canine heart failure model. Cardiovasc Res. 2005; 66:472–481. [PubMed: 15914112]
8. Chandler NJ, Greener ID, Tellez JO, Inada S, Musa H, Molenaar P, DiFrancesco D, Baruscotti M, Longhi R, Anderson RH, Billeter R, Sharma V, Sigg DC, Boyett MR, Dobrzynski H. Molecular architecture of the human sinus node: insights into the function of the cardiac pacemaker. Circulation. 2009; 119:1562–1575. [PubMed: 19289639]
9. Wahl-Schott C, Biel M. HCN channels: structure, cellular regulation and physiological function. Cell Mol Life Sci. 2009; 66:470–794. [PubMed: 18953682]
10. Fenske S, Krause SC, Hassan SI, Becirovic E, Auer F, Bernard R, Kupatt C, Lange P, Ziegler T, Wotjak CT, Zhang H, Hammelmann V, Paparizos C, Biel M, Wahl-Schott CA. Sick sinus syndrome in HCN1-deficient mice. Circulation. 2013; 128:2585–2594. [PubMed: 24218458]
11. Lou Q, Hansen BJ, Fedorenko O, Csepe T, Kalyanasundaram A, Li N, Hage L, Glukhov AV, Billman GE, Weiss R, Mohler PJ, Gyorke S, Biesiadecki BJ, Carnes C, Fedorov VV. Upregulation of Adenosine A1 Receptors Facilitates Sinoatrial Node Dysfunction in Chronic Canine Heart Failure by Exacerbating Nodal Conduction Abnormalities Revealed by Novel Dual-Sided Intramural Optical Mapping. Circulation. 2014; 130:315–324. [PubMed: 24838362]
12. Verkerk AO, Wilders R, Coronel R, Ravesloot JH, Verheijck EE. Ionic remodeling of sinoatrial node cells by heart failure. Circulation. 2003; 108:760–766. [PubMed: 12885752]
13. Verkerk AO, Wilders R, van Borren MM, Peters RJ, Broekhuis E, Lam K, Coronel R, de Bakker JM, Tan HL. Pacemaker current (I(f)) in the human sinoatrial node. Eur Heart J. 2007; 28:2472–2478. [PubMed: 17823213]
14. Verkerk AO, Wilders R. Pacemaker Activity of the Human Sinoatrial Node: An Update on the Effects of Mutations in HCN4 on the Hyperpolarization-Activated Current. Int J Mol Sci. 2015; 16:3071–3094. [PubMed: 25642760]
15. Schweizer PA, Schroter J, Greiner S, Haas J, Yampolsky P, Mereles D, Buss SJ, Seyler C, Bruehl C, Draguhn A, Koenen M, Meder B, Katus HA, Thomas D. The symptom complex of familial sinus node dysfunction and myocardial noncompaction is associated with mutations in the HCN4 channel. J Am Coll Cardiol. 2014; 64:757–767. [PubMed: 25145518]
16. Hansen BJ, Zhao J, Csepe TA, Moore BT, Li N, Jayne LA, Kalyanasundaram A, Lim P, Bratasz A, Powell KA, Simonetti OP, Higgins RS, Kilic A, Mohler PJ, Janssen PM, Weiss R, Hummel JD, Fedorov VV. Atrial fibrillation driven by micro-anatomic intramural re-entry revealed by

simultaneous sub-epicardial and sub-endocardial optical mapping in explanted human hearts. Eur Heart J. Jun 8.2015 [Epub ahead of print].

17. Sanchez-Quintana D, Cabrera JA, Farre J, Climent V, Anderson RH, Ho SY. Sinus node revisited in the era of electroanatomical mapping and catheter ablation. Heart. 2005; 91:189–194. [PubMed: 15657230]
18. Fedorov VV, Glukhov AV, Chang R. Conduction barriers and pathways of the sinoatrial pacemaker complex: their role in normal rhythm and atrial arrhythmias. Am J Physiol Heart Circ Physiol. 2012; 302:H1773–H1783. [PubMed: 22268110]
19. Csepe TA, Kalyanasundaram A, Hansen BJ, Zhao J, Fedorov VV. Fibrosis: a structural modulator of sinoatrial node physiology and dysfunction. Front Physiol. 2015; 6:37. [PubMed: 25729366]
20. Nixon BR, Thawornkaiwong A, Jin J, Brundage EA, Little SC, Davis JP, Solaro RJ, Biesiadecki BJ. AMP-activated protein kinase phosphorylates cardiac troponin I at Ser-150 to increase myofilament calcium sensitivity and blunt PKA-dependent function. J Biol Chem. 2012; 287:19136–19147. [PubMed: 22493448]
21. Liu J, Dobrzynski H, Yanni J, Boyett MR, Lei M. Organisation of the mouse sinoatrial node: structure and expression of HCN channels. Cardiovasc Res. 2007; 73:729–738. [PubMed: 17222809]
22. Bucchi A, Barbuti A, DiFrancesco D, Baruscotti M. Funny Current and Cardiac Rhythm: Insights from HCN Knockout and Transgenic Mouse Models. Front Physiol. 2012; 3:240. [PubMed: 22783204]
23. Cappato R, Castelvecchio S, Ricci C, Bianco E, Vitali-Serdoz L, Gnecchi-Ruscone T, Pittalis M, De AL, Baruscotti M, Gaeta M, Furlanello F, Di FD, Lupo PP. Clinical efficacy of ivabradine in patients with inappropriate sinus tachycardia: a prospective, randomized, placebo-controlled, double-blind, crossover evaluation. J Am Coll Cardiol. 2012; 60:1323–1329. [PubMed: 22981555]
24. Borer JS, Fox K, Jaillon P, Lerebours G. Antianginal and antiischemic effects of ivabradine, an I(f) inhibitor, in stable angina: a randomized, double-blind, multicentered, placebo-controlled trial. Circulation. 2003; 107:817–823. [PubMed: 12591750]
25. Lakatta EG, Maltsev VA, Vinogradova TM. A coupled SYSTEM of intracellular Ca2+ clocks and surface membrane voltage clocks controls the timekeeping mechanism of the heart's pacemaker. Circ Res. 2010; 106:659–673. [PubMed: 20203315]
26. Herrmann S, Layh B, Ludwig A. Novel insights into the distribution of cardiac HCN channels: an expression study in the mouse heart. J Mol Cell Cardiol. 2011; 51:997–1006. [PubMed: 21945247]
27. Brioschi C, Micheloni S, Tellez JO, Pisoni G, Longhi R, Moroni P, Billeter R, Barbuti A, Dobrzynski H, Boyett MR, DiFrancesco D, Baruscotti M. Distribution of the pacemaker HCN4 channel mRNA and protein in the rabbit sinoatrial node. J Mol Cell Cardiol. 2009; 47:221–227. [PubMed: 19394343]
28. Chandler N, Aslanidi O, Buckley D, Inada S, Birchall S, Atkinson A, Kirk D, Monfredi O, Molenaar P, Anderson R, Sharma V, Sigg D, Zhang H, Boyett M, Dobrzynski H. Computer three-dimensional anatomical reconstruction of the human sinus node and a novel paranodal area. Anat Rec (Hoboken). 2011; 294:970–979. [PubMed: 21538926]
29. Ludwig A, Budde T, Stieber J, Moosmang S, Wahl C, Holthoff K, Langebartels A, Wotjak C, Munsch T, Zong X, Feil S, Feil R, Lancel M, Chien KR, Konnerth A, Pape HC, Biel M, Hofmann F. Absence epilepsy and sinus dysrhythmia in mice lacking the pacemaker channel HCN2. EMBO J. 2003; 22:216–224. [PubMed: 12514127]
30. Atkinson AJ, Logantha SJ, Hao G, Yanni J, Fedorenko O, Sinha A, Gilbert SH, Benson AP, Buckley DL, Anderson RH, Boyett MR, Dobrzynski H. Functional, anatomical, and molecular investigation of the cardiac conduction system and arrhythmogenic atrioventricular ring tissue in the rat heart. J Am Heart Assoc. 2013; 2:e000246. [PubMed: 24356527]
31. Li N, Hansen BJ, Csepe TA, Jayne L, Zhao J, Moore B, Higgins RS, Weiss R, Kilic A, Rosen MR, Mohler PJ, Biesiadecki BJ, Janssen PM, Fedorov VV. Functional and Molecular Characteristics of the Latent Atrial Pacemaker Clusters in Explanted Human Hearts. Circulation. 2014; 130:A18888.
32. DiFrancesco D. Serious workings of the funny current. Prog Biophys Mol Biol. 2006; 90:13–25. [PubMed: 15975637]

33. Bucchi A, Tognati A, Milanesi R, Baruscotti M, DiFrancesco D. Properties of ivabradine-induced block of HCN1 and HCN4 pacemaker channels. J Physiol. 2006; 572:335–346. [PubMed: 16484306]
34. Plotnikov AN, Bucchi A, Shlapakova I, Danilo P Jr. Brink PR, Robinson RB, Cohen IS, Rosen MR. HCN212-channel biological pacemakers manifesting ventricular tachyarrhythmias are responsive to treatment with I(f) blockade. Heart Rhythm. 2008; 5:282–288. [PubMed: 18242555]
35. Moosmang S, Stieber J, Zong X, Biel M, Hofmann F, Ludwig A. Cellular expression and functional characterization of four hyperpolarization-activated pacemaker channels in cardiac and neuronal tissues. Eur J Biochem. 2001; 268:1646–1652. [PubMed: 11248683]
36. Cerbai E, Mugelli A. I(f) in non-pacemaker cells: role and pharmacological implications. Pharmacol Res. 2006; 53:416–423. [PubMed: 16713285]
37. Fenske S, Mader R, Scharr A, Paparizos C, Cao-Ehlker X, Michalakis S, Shaltiel L, Weidinger M, Stieber J, Feil S, Feil R, Hofmann F, Wahl-Schott C, Biel M. HCN3 contributes to the ventricular action potential waveform in the murine heart. Circ Res. 2011; 109:1015–1023. [PubMed: 21903939]
38. Schweizer PA, Yampolsky P, Malik R, Thomas D, Zehelein J, Katus HA, Koenen M. Transcription profiling of HCN-channel isotypes throughout mouse cardiac development. Basic Res Cardiol. 2009; 104:621–629. [PubMed: 19421833]
39. Stillitano F, Lonardo G, Giunti G, Del LM, Coppini R, Spinelli V, Sartiani L, Poggesi C, Mugelli A, Cerbai E. Chronic atrial fibrillation alters the functional properties of If in the human atrium. J Cardiovasc Electrophysiol. 2013; 24:1391–1400. [PubMed: 23869794]
40. Stillitano F, Lonardo G, Zicha S, Varro A, Cerbai E, Mugelli A, Nattel S. Molecular basis of funny current (If) in normal and failing human heart. J Mol Cell Cardiol. 2008; 45:289–299. [PubMed: 18556018]
41. Cai J, Yi FF, Li YH, Yang XC, Song J, Jiang XJ, Jiang H, Lin GS, Wang W. Adenoviral gene transfer of HCN4 creates a genetic pacemaker in pigs with complete atrioventricular block. Life Sci. 2007; 80:1746–1753. [PubMed: 17382969]
42. Plotnikov AN, Shlapakova I, Szabolcs MJ, Danilo P Jr. Lorell BH, Potapova IA, Lu Z, Rosen AB, Mathias RT, Brink PR, Robinson RB, Cohen IS, Rosen MR. Xenografted adult human mesenchymal stem cells provide a platform for sustained biological pacemaker function in canine heart. Circulation. 2007; 116:706–713. [PubMed: 17646577]
43. Tse HF, Xue T, Lau CP, Siu CW, Wang K, Zhang QY, Tomaselli GF, Akar FG, Li RA. Bioartificial sinus node constructed via in vivo gene transfer of an engineered pacemaker HCN Channel reduces the dependence on electronic pacemaker in a sick-sinus syndrome model. Circulation. 2006; 114:1000–1011. [PubMed: 16923751]

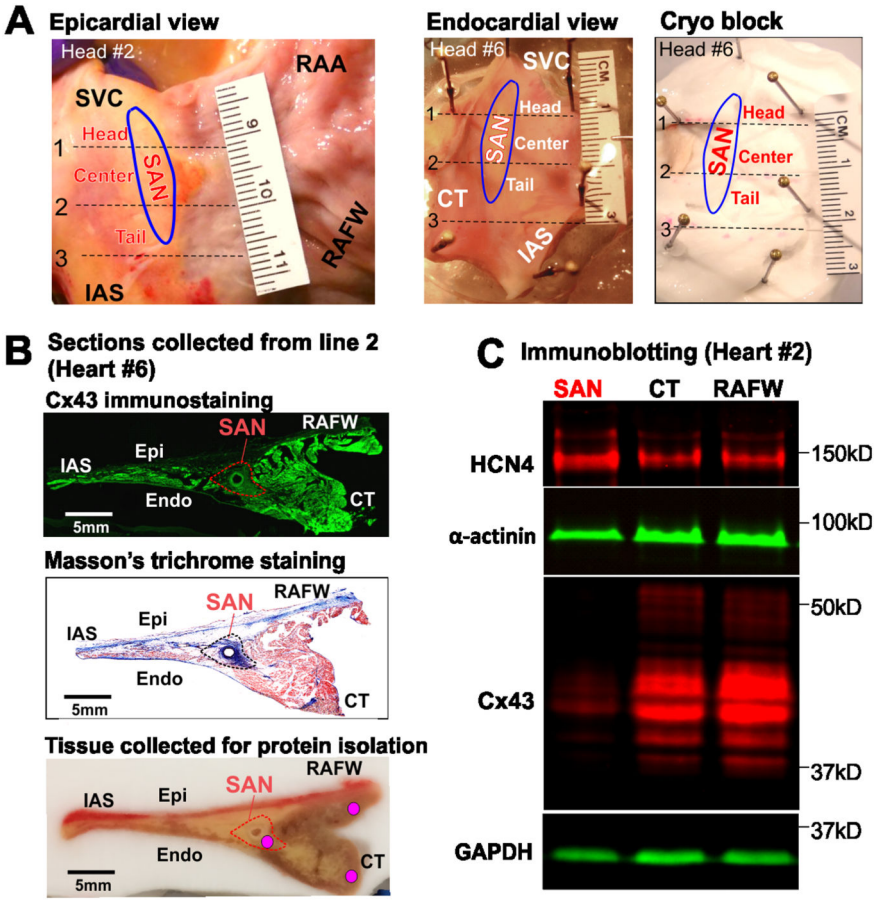

Figure 1.

SAN localization and tissue dissection. (**A**) Epicardial and endocardial views of the human SAN preparation with SAN outlined in blue. Black dashed lines 1-3 indicate the dissection locations. (**B**) Transmural sections collected adjacent to line 2. Top: Cx43 (green signal) immunolabeling shows no positive staining in the SAN area. Images of sections were taken using a high resolution scanner (20x). Middle: Masson's trichrome staining displays SAN as the dense fibrotic and cardiomyocyte compact region around the SAN artery. Cardiac myocytes were stained red and connective tissue was stained blue. Bottom: photograph of the cross section of the SAN preparation. Pink dots show the locations where tissue was collected for protein isolation. (**C**) Immunoblot shows protein expression of HCN4, α-actinin, Cx43 and GAPDH. Endo, endocardial; Epi, epicardial; SVC, superior vena cava; CT, crista terminalis; IAS, inter-atrial septum; RAA, right atrial appendage; RAFW, right atrial free wall; SAN, sinoatrial node.

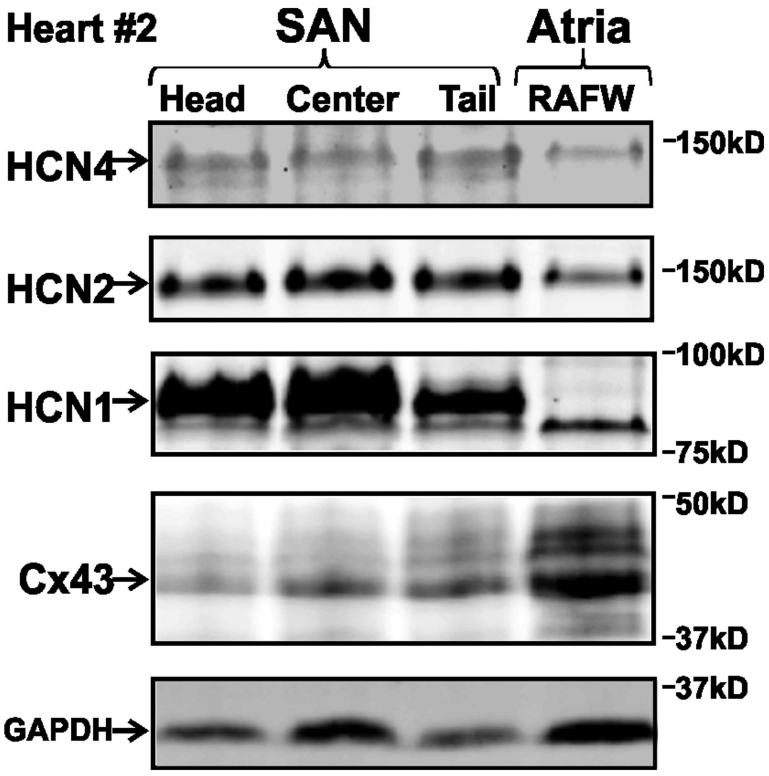

Figure 2.

Representative immunoblot for HCN protein distribution in human SAN head, center, tail and RAFW from Heart #2. HCN4 and HCN2 are displayed at about 150kDa. A 90kDa band corresponds to the mature glycosylated HCN1 protein and an 85kDa band represents a non-specific band. There are multiple bands around 43kDa corresponding to different phosphorylated and dephosphorylated isoforms of Cx43.

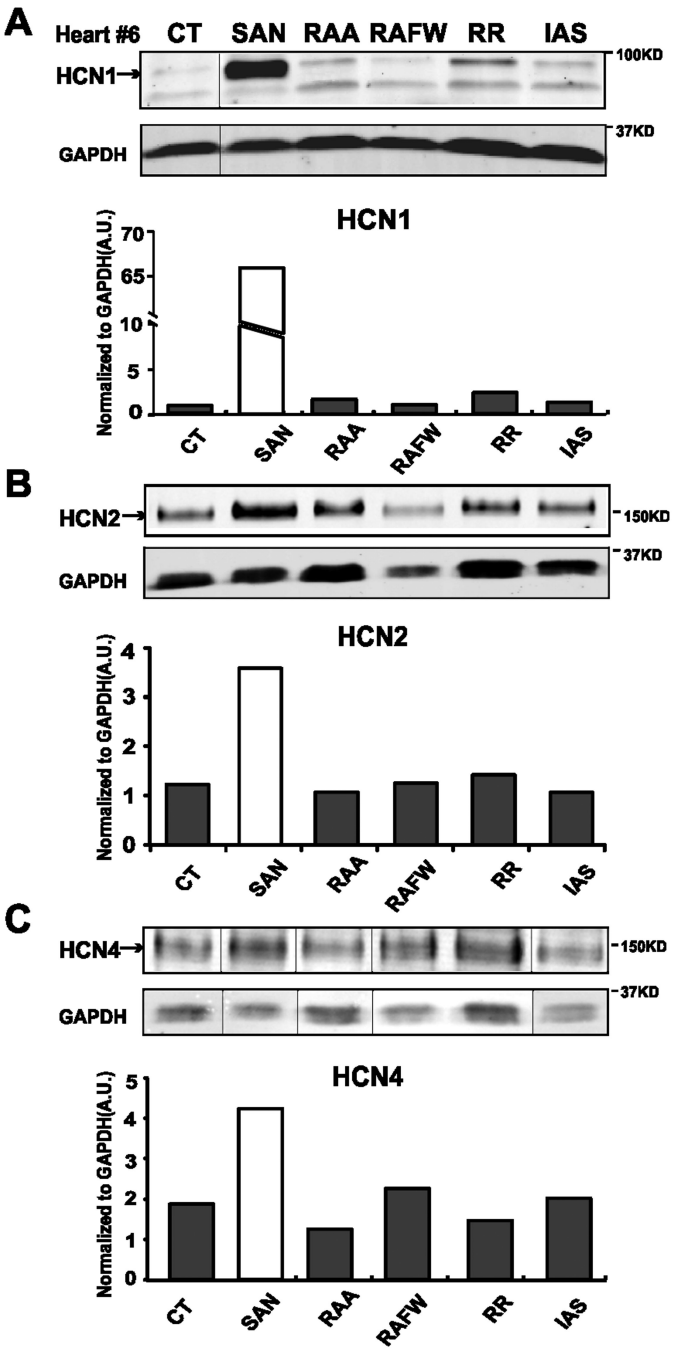

Figure 3.

HCN isoform expression pattern in human SAN and adjacent atrial tissues. Immunoblot showing protein expression level of (**A**) HCN1, (**B**) HCN2, and (**C**) HCN4 in human SAN and adjacent atria (Heart #6). HCN band density normalized to GAPDH (arbitrary units) presented in graphs. In panel C, all the samples were run on the same gel, however to keep consistent with panel A and B, regions were cut and reordered. RR, right atrioventricular ring. Other abbreviations as in Figure 1.

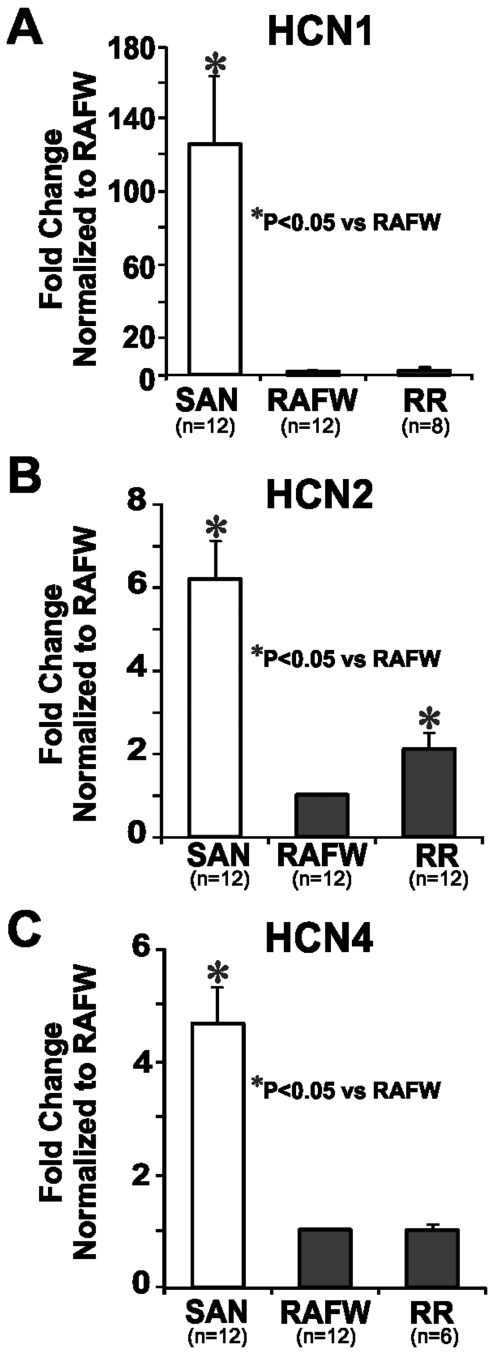

Figure 4.

Bar graphs showing the relative value of (**A**) HCN1, (**B**) HCN2, and (**C**) HCN4 protein expression as measured by immunoblotting band density in human SAN, RAFW and RR. GAPDH normalized band density is shown in Mean±SEM and normalized to the value of the RAFW.

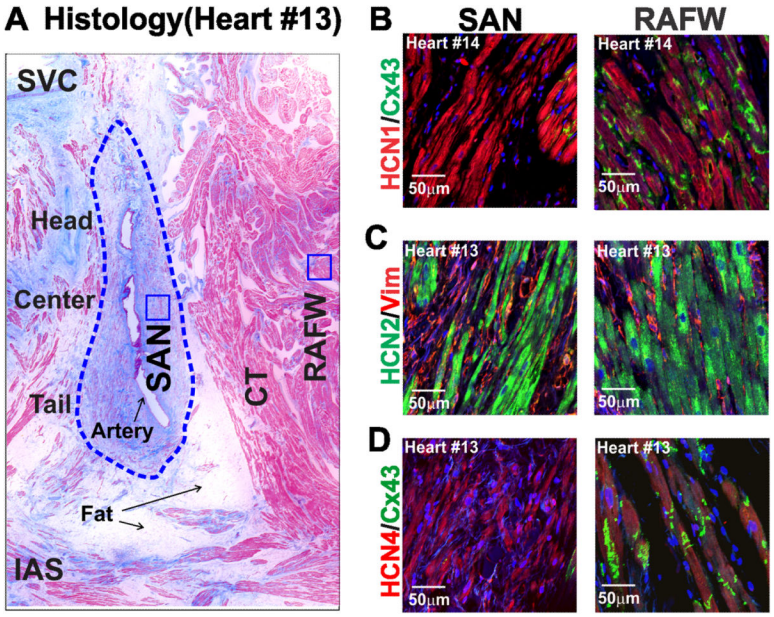

Figure 5.

Masson's trichrome staining and HCN, Cx43 and Vimentin immunolabeling of the human SAN and RAFW (Heart #13 and #14). (**A**) Masson's trichrome stained section of human SAN preparation with SAN outlined in blue. The blue squares indicated the locations where the high-resolution images in B-D were taken from the sister-sections. (**B**) HCN1 (red) signal labels the myocytes and Cx43 (green) signal displays the cell connections between myocytes. Cx43 signal is negative in the SAN area. (**C**) HCN2 (green) signal labels the cardiomyocytes which is smaller in size in SAN area than in RAFW. Vimentin (Vim, red) signal shows the fibroblasts which are abundant in the SAN area. (**D**) HCN4 (red) and Cx43 (green) double staining labels the cardiomyocytes and connexin separately.

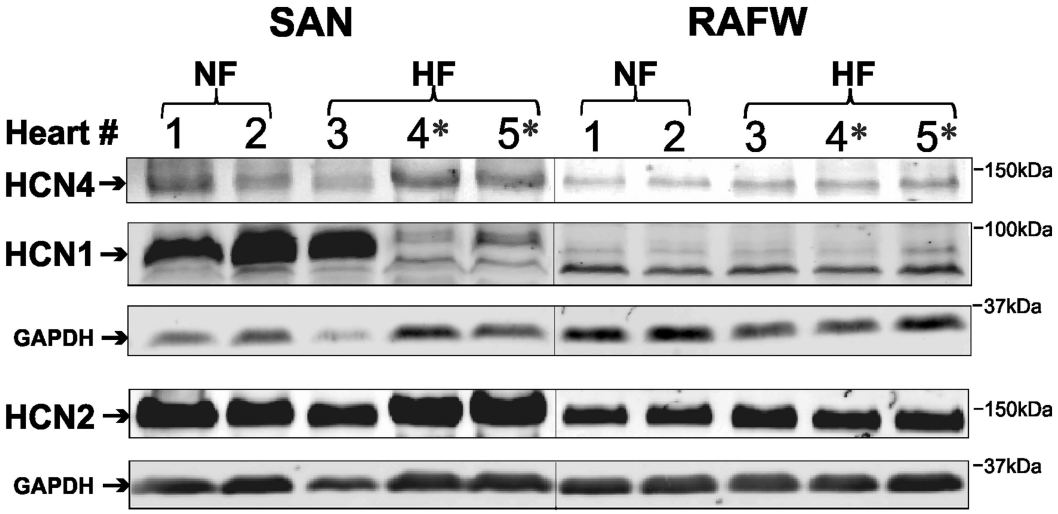

Figure 6.

Expression pattern of HCN1, HCN2 and HCN4 protein in human SAN and RAFW from control and diseased hearts. Immunoblot showed Heart #4 and #5 (ischemic HF hearts indicated by *) had lower HCN1 expression in SAN than Heart #3 (non-ischemic HF) while HCN2 and HCN4 expression was still well-preserved in Heart #4 and #5 SAN.

Table 1

Human heart information

Heart No.	Code No.	Age	Gender	Source	Heart Failure	Main Diagnoses	Device	H.W. (g)
1	712301	67	Male	LOOP	−	Blunt Injury, HTN	None	527
2	809108	60	Male	LOOP	−	Cardiac Arrest, HTN, DM	None	842
3	911614	65	Male	OSU	+	Non Ischemic HF (Transplant), AF	CRT, LVAD	716
4	774694	50	Female	OSU	+	Ischemic HF (Transplant), CAD	None	486
5	674541	64	Male	LOOP	+	Stroke, Ischemic HF, CAD, HTN, DM	ICD, LVAD	599
6	600245	51	Female	LOOP	−	CVA/ICH	None	507
7	768159	44	Male	LOOP	−	Cardiac Arrest*, VF, DM	None	279
8	845013	26	Male	LOOP	−	Cardiac Arrest, VT/VF, VSD	PM	497
9	380071	43	Female	LOOP	−	Respiratory Arrest*, CAD, HTN, DM, Morbid Obesity,	None	603
10	574165	62	Male	LOOP	−	Blunt Injury, AF	None	584
11	724569	64	Male	OSU	+	Non Ischemic HF(Transplant), AF, VT, HTN, Hypothyroidism	PM	636
12	971258	57	Male	OSU	+	Ischemic HF(Transplant), CAD, MI, AF	ICD, LVAD	619
13	168021	62	Female	LOOP	−	CVA/ICH, CAD, HTN, DM	None	896
14	921821	22	Male	LOOP	−	Cardiac Arrest, VT, DM	None	383

The causes of death (transplantation) were indicated by underline.

AF = Atrial Fibrillation; CAD = Coronary Artery Disease; CRT = Cardiac resynchronization therapy; CVA/ICH = Cardiovascular Attack/ Intracranial Hemorrhage; DM = Diabetes Mellitus; HF =Heart Failure; HTN= Hypertension; H.W. = Heart Weight; ICD = Implantable Cardiac Defibrillator; LOOP = Lifeline of Ohio Organ Procurement Organization; LVAD = Left Ventricular Assist Device; OSU = The Ohio State University Wexner Medical Center; PM = Pacemaker; VF = Ventricular Fibrillation; VSD = Ventricular Septal Defect; VT = Ventricular Tachycardia. .

*indicates the patient had longer than 20 minutes of cardiac down time